ENERGY EFFICIENCY OF COMMERCIALLY USED MPPT ALGORITHMS IN SOLAR ENERGY HARVESTING

Hamed Osouli Tabrizi[1*], Murat Fahrioglu[2]
1- Sustainable Environment and Energy Systems, Middle East Technical University, Northern Cyprus Campus, Kalkanli, Guzelyurt Mersin 10, Turkey
2- Electrical and Electronics Engineering Dept, Middle East Technical University, Northern Cyprus Campus, Kalkanli, Guzelyurt Mersin 10, Turkey
Corresponding author: Hamed Osouli Tabrizi, e-mail: hamed.tabrizi@metu.edu.tr

REFERENCE NO
EFFN-01

Keywords:
Solar Energy Harvesting, Energy Efficiency, MPPT

ABSTRACT

In order to harvest maximum energy under continuously changing temperature and irradiation, Maximum Power Point Tracking (MPPT) circuits must be exploited for solar energy harvesting. Different MPPT algorithms are proposed in the literature to provide optimality under various conditions and increase the convergence speed, robustness and reliability of the system. Energy efficiency of these algorithms is less investigated. In this paper energy efficiency of two most commercially and commonly used MPPT algorithms is studied. Closed loop behaviour of fixed step size and adaptive step size perturb and observe algorithms is simulated assuming three different irradiation and temperature change scenarios. A new energy efficiency metric is introduced which separately considers energy efficiency during transition and in maximum power point. Adaptive algorithm is found to be in average 14.76% more energy efficient than fixed step size algorithm.

1. INTRODUCTION

Recently, solar energy has been among major sources of renewable energy both in high power generation and low power applications such as stand-alone domestic solar cells, and battery chargers. Solar energy conversion is known to be less efficient in comparison to other counterparts [1-2]. For a solar PV cell, variation in irradiance, ambient temperature or load dramatically affects I-V curve which in turn shifts Maximum Power Point (MPP) in the P-V curve. Therefore Maximum Power Point Tracking (MPPT) circuitry is an inessential block in solar energy harvesting units to maximize power efficiency by tracking output impedance of the cell [3-5]. Figure 1 depicts block diagram of a typical solar energy harvesting unit which is composed of a boost converter and an MPPT block. MPPT block adjusts input impedance of the boost converter to match output impedance of the cell by sensing output current and/or voltage of the cell.

In [4], [7], [8], [9], [18] comparative studies have been carried out to analyse different MPPT algorithms proposed in the literature. These studies include performance comparison of different types of MPPT algorithms particularly two most commercially used MPPT algorithms, Perturb and observe (P&O) and incremental conductance (IC). The most commercially used algorithm is P&O due to its simplicity and accuracy [7-9]. Output voltage and current values of the solar PV cell are measured after intentionally perturbing the voltage. After each perturbation and measurement, processing unit calculates delivered power before and after perturbation and generates a control signal which is usually a pulse width modulated (PWM) by comparing the two power values [10-16]. This algorithm is discussed in detail in section IV.

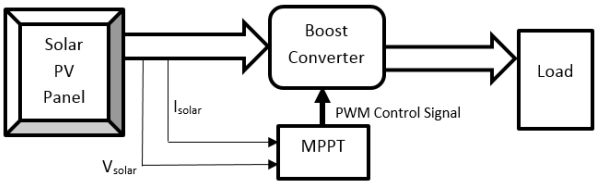

Figure 1. Block Diagram of a typical solar energy harvesting unit. MPPT block adjusts input impedance of the boost converter to match with output impedance of the cell by sensing output current and voltage of the cell

In [11] a comparison between two implementation techniques of P&O

algorithms, reference voltage and direct duty ratio perturbation, is carried out. Direct duty ratio perturbation is reported to be more stable, more efficient and less sensitive to noise. Direct duty ratio perturbation can be implemented using fixed step size or adaptive (variable) step size. There has been no analytical study between these two pervasive MPPT algorithms. In this paper energy efficiency of these two algorithms is investigated. MATLAB is used to simulate closed loop behaviour of these two algorithms under three different irradiation and temperature change scenarios.

The rest of the paper is organized as follows. In section 2 mathematical model of solar PV cell is investigated. In section 3 boost converter model is briefly discussed. In section 4 different types of perturb and observe algorithm are discussed. In section 5, a new metric for energy efficiency is introduced which separately considers energy efficiency during transition and in maximum power point . Section 6 depicts simulation results for fixed and adaptive step size P&O algorithms.

2. SOLAR PV CELL MODEL

Solar PV cells act as current sources since they convert photons to carrying electrons. In [19] a commonly used one-diode model is described and its parameter values are given such that the model matches with commercial solar panel products. This model is shown in Figure 2.

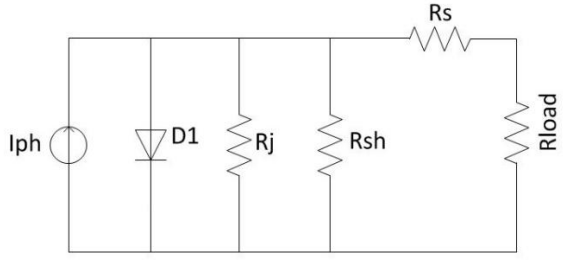

Figure 2: One-Diode Circuit model for Solar PV cell

In this model Iph is cell photo current, Rj is nonlinear impedance of p-n junction Rsh and Rs are intrinsic shunt and series resistance. Usually for regular panels Rs is very small and Rsh is so high that can be neglected. The overall current of the solar cell in a network involving n_p cells in parallel and n_s cells in series is defined by (1)

$$I_o = n_p I_{ph} - n_p I_{rs}\left[e^{\left(\frac{q}{kTA}\frac{V_0}{n_s}\right)} - 1\right] \quad (1)$$

Where I_{rs} is the current without radiation described in (2) and I_{ph} is the current with radiation described by (3).

$$I_{rs} = I_{rr}\left[\frac{T}{T_r}\right]^3 e^{\left(\frac{qE_G}{kQA}\left[\frac{1}{T_r}-\frac{1}{T}\right]\right)} \quad (2)$$

$$I_{ph} = [I_{src} + k_i(T - T_r)]\frac{s}{100} \quad (3)$$

Definition and values of different parameters in equation 1, 2 and 3 are reported in detail in [19]. This model is used to simulate close loop behaviour of the system.

3. DC-DC CONVERTER MODEL

Figure 3 shows schematic of a boost converter. Operating point of a solar PV cell in the closed loop system is determined by the input impedance of the boost converter. Output voltage and input impedance of the boost converter is defined by (4) and (5).

$$V_{out,DC} = \frac{V_{in}}{1-D} \quad (4)$$

$$R_{in} = (1-D)^2 R_{Load} \quad (5)$$

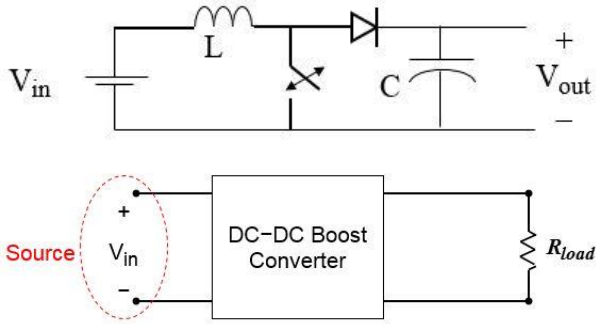

Figure 3: A typical boost converter. $V_{out,DC} = \frac{V_{in}}{1-D}$

4. PERTURB AND OBSERVE ALGORITHM

In the “perturb” cycle of this algorithm, a small change is applied by altering the duty cycle of the DC-DC coverter. In the “observe” cycle, output power is calculated using

voltage and current sensors data and compared with its value before perturbation. Table. 1 summarizes the logic behind perturb and observe method.

Table 1: the logic behind perturb and observe method

Perturbation	Change in power	Next perturbation
Positive	Positive	Positive
Positive	Negative	Negative
Negative	Positive	Negative
Negative	Negative	Positive

In order to continually detect the maximum power point this algorithm should be perturbing all the time. On the other hand there are many adaptive step size algorithms introduced [20-23]. In the algorithm introduced in [21] which is optimized for being implemented in commercial products step size can be adjusted based on the proximity of the solar PV operating point to the maximum power point. If the perturbed point is diverging from the maximum power point the step size is increased otherwise step is decreased. This algorithm is reported to be fast with minimum implementation hardware requirements. In addition, this algorithm offers feedback with two control loops which offers better performance under partial conditions and current load step.

In addition to perturb and observe algorithm there are many maximum power point tracking algorithms introduced in the literature such as Fractional open circuit Voltage [24], Incremental Conductance [25] fuzzy logic [26] and neural network [27] to overcome different drawbacks of other methods. However most of these are not applicable in standalone low power applications mainly because of considerable hardware implementations. [7]

5. ENERGY EFFICIENCY METRIC AND COMPARISON OF ALGORITHMS

MPPT algorithm has a major effect on performance of the solar cell energy harvesting system. In order to investigate energy efficiency of MPPT three dominant factors in the online tracking procedure should be addressed. i) *Convergence Speed* which can be defined as the time required for the algorithm to find the maximum power point each time there is a change in the temperature or irradiation density. Since delay inversely affects efficiency, faster algorithms are required in order to achieve higher efficiencies. ii) *Power consumption of the MPP tracker unit*. An MPPT circuit can be one of the most power hungry blocks in the harvesting system specially if implemented with analogue circuits. For high power Energy harvesting however power consumption of the MPPT circuit is negligible. [17] iii) *Oscillation in the Maximum Power Point*. Perturb and observe algorithm is based on constant perturbation. Oscillation is not desired when the system is working in the maximum power point due to considerable decrease in system efficiency.

Efficiency has direct relation with Convergence speed and invers relation with hardware energy consumption and oscillation. This is shown in the proposed metric by equation (6) to (9). Considering these facts efficiency can be calculated in terms of the generated energy using an MPPT over Total energy generation capability of cell. Total energy generation capability of the cell can be calculated knowing the temperature and irradiation profile together with cell efficiency.

$$\eta_T = \frac{\int^{T_T} P_T \, dt}{\int^{T} P_{Max} \, dt} \tag{6}$$

$$\eta_{MPP} = \frac{\int^{T_{MPP}} P_{MPP} \, dt}{\int^{T} P_{Max} \, dt} \tag{7}$$

$$\eta_{circ} = -\frac{\int^{T_{Total}} P_{circ} \, dt}{\int^{T} P_{Max} \, dt} \tag{8}$$

$$MMPT_{EEF} = \eta_T + \eta_{MPP} + \eta_{circ} \tag{9}$$

Where $MMPT_{EEF}$ is the energy efficiency metric of MMP tracking system, T_T is transition time which is the time spent for the controller to settle to the maximum power point, P_{max} is the maximum power that solar PV can deliver in the maximum power point, P_T stands for power generated during transition stage, T_{MPP} being the time that

system is operating in the maximum power point, P_{MPP} is power generated when the system is operating in the maximum power point, P_{circ} stands for power dissipated by MPPT circuit and finally T is the total time.
This metric is calculated to compare fixed and variable size MMPT algorithms in terms of their energy efficiency.

6. SIMULATION AND COMPARISON RESULTS

Figure 4 and 5 show solar panel I-V curves using the model in section 2 in different irradiation and temperature conditions respectively. Figure 6 and 7 show solar panel I-V curves using the same model in different irradiation and temperature conditions. Different irradiation levels severely affect output current and therefore power of the cell. Increase in temperature inversely affects solar cell power generation.

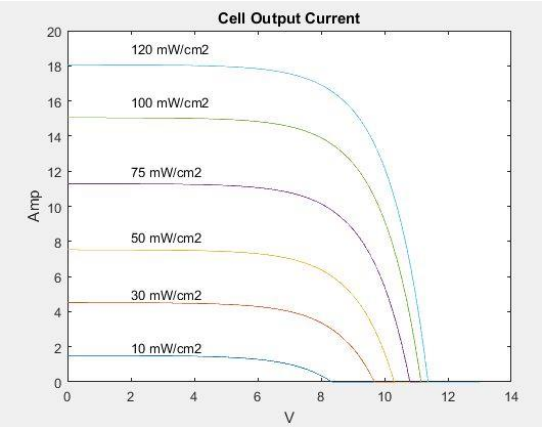

Figure 4: I-V curves under different irradiation conditions

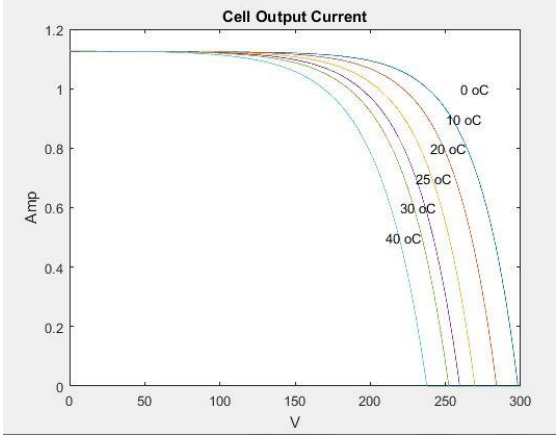

Figure 5: I-V curves under different Temperature conditions

All simulations are done for one hour duration. The time step for simulation is one minute. Three different scenarios are taken into account. Firs scenario assumes that irradiation doesn't change during one hour of simulation.

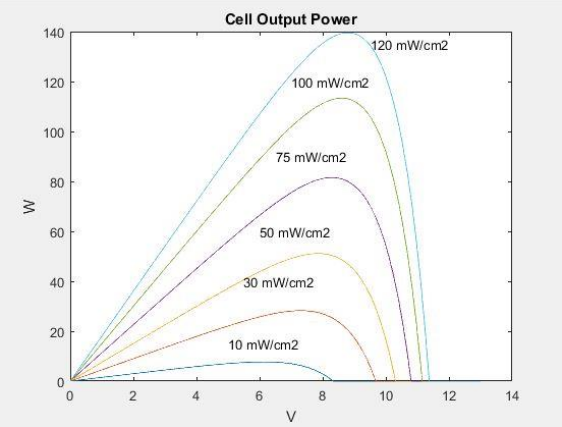

Figure 6: P-V curves under different irradiation conditions

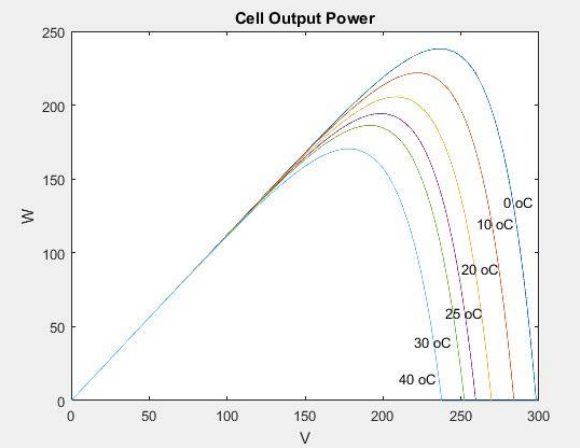

Figure 7: P-V curves under different Temperature conditions

In the second scenario irradiation is assumed to reduce to half in the second 30 minutes of the simulation similar to the effect of long shading due to the presence of clouds. In the Third scenario the assumption is short shading because of passing clouds that take place for only five minutes. Temperature is considered to be fixed for all scenarios. The effect of MMPT algorithm with fixed step size based on first scenario is shown in figure 8 and 9. Figure 8 shows output power with 4 different step sizes for the fixed size algorithm. Figure 9 shows the switching activity of the circuit which is the result of control unit to adjust duty cycle as control signal.

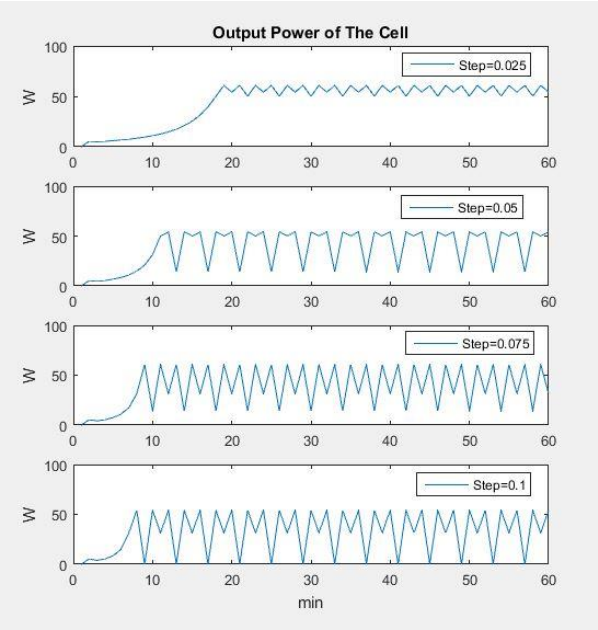

Figure 8: output power in one hour assuming constant irradiation and temperature during simulation with 4 different step size for the fixed size algorithm

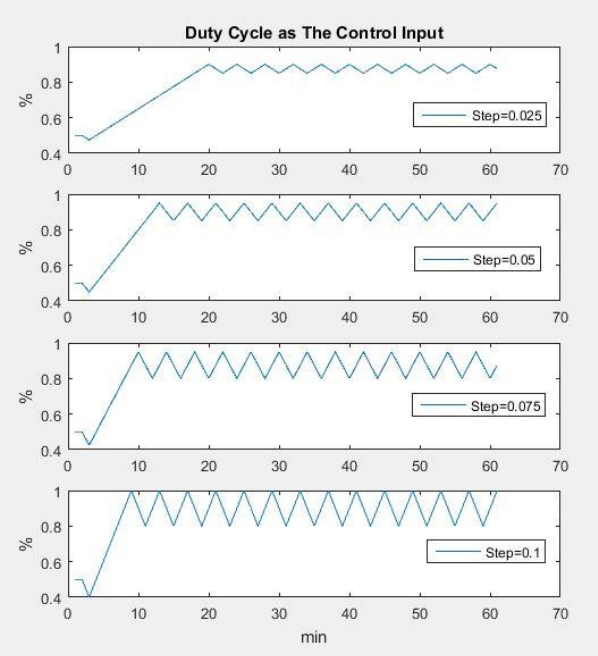

Figure 9: output power in one hour assuming constant irradiation and temperature during simulation with 4 different step size for the fixed size algorithm

Figure 10 and 11 show the same simulations for the second scenario that assumes a significant drop in the second half of simulation period due to presence of dense cloud.

Figure 12 and 13 are the simulation results for the third scenario in which there is only a very fast change in irradiation amount due to passing clouds for 5 minutes. Bigger step size helps faster detection of rapid ambient condition changes.

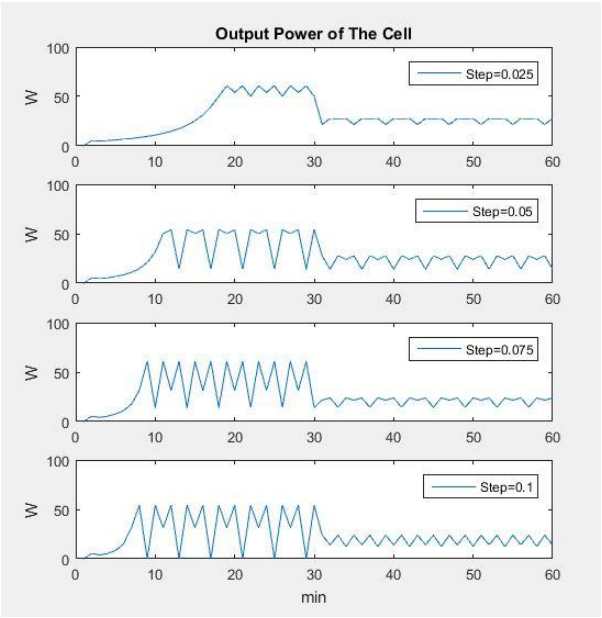

Figure 10: output power in one hour assuming irradiation cut into half during second half of the simulation with 4 different step size for the fixed size algorithm

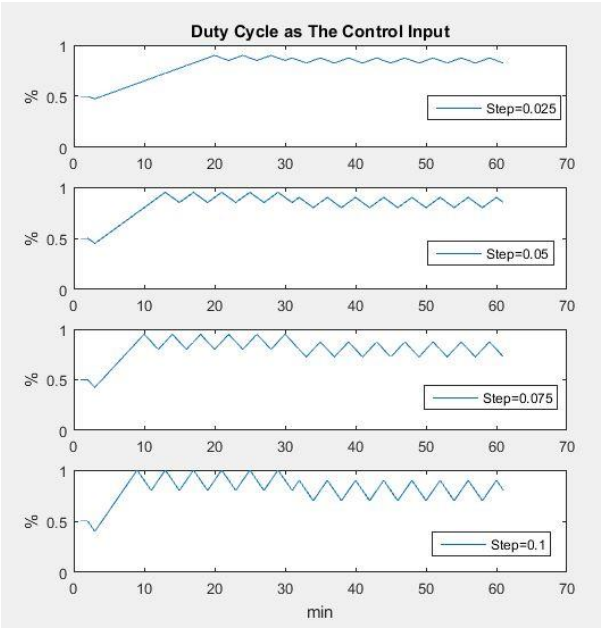

Figure 11: Duty Cycle in one hour assuming irradiation cut into half during second half of the simulation with 4 different step size for the fixed size algorithm

On the other hand, very big step size causes oscillation that decreases the average output power. In addition, for smaller step sizes there is less switching activity which can help to reducing the dynamic power consumption.

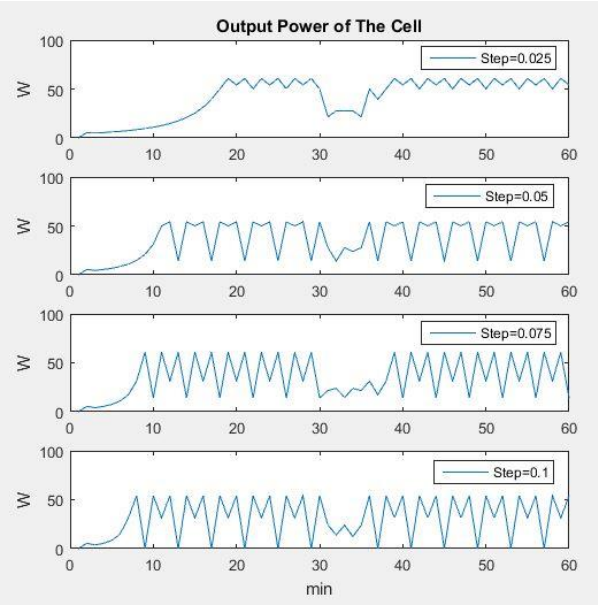

Figure 12: output power in one hour assuming a 5 minute-decrease in the amount of the irradiation during 1 hour of simulation with 4 different step size for the fixed size algorithm

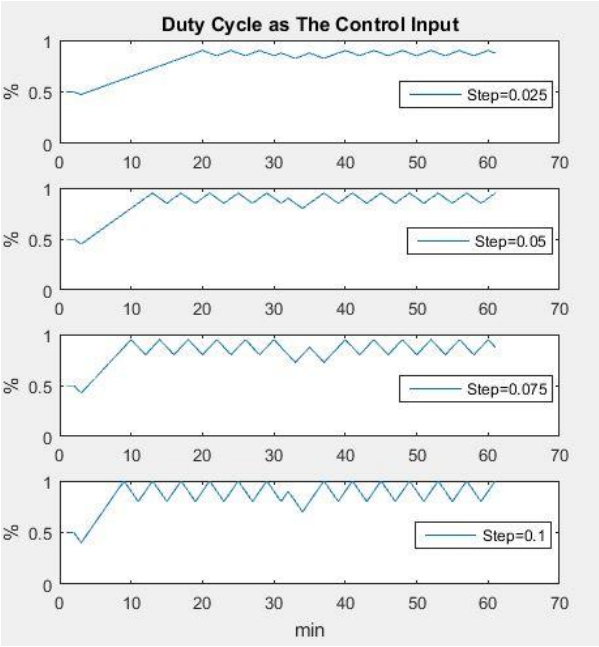

Figure 13: Duty Cycle in one hour assuming a 5 minute-decrease in the amount of the irradiation during 1 hour of simulation with 4 different step size for the fixed size algorithm

Figure 14 and 15 show the output power of the solar cell for the first scenario by utilizing adaptive method. Adaptive algorithm sets a relatively big step size in the beginning of the tracking process then decreased step size as it reaches maximum power point. When detecting any change in the conditions step size reset to its initial value making algorithm sweep a large area to find the next maximum power point.

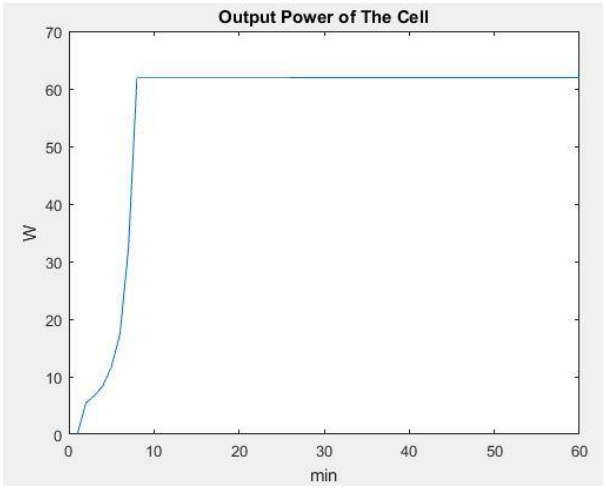

Figure 14: Output power in one hour assuming constant irradiation and temperature during simulation for the variable step size algorithm

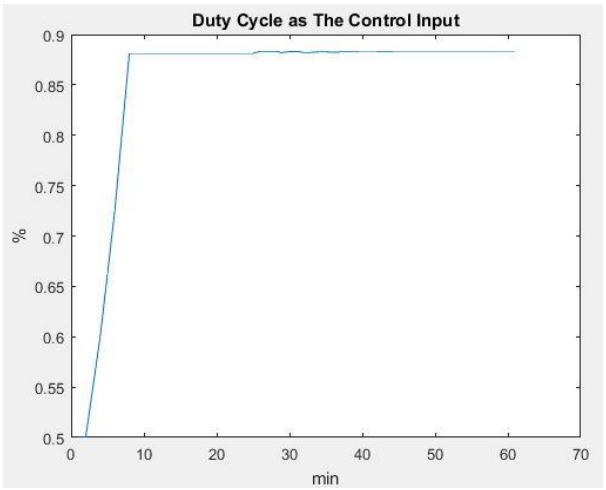

Figure 15: Duty Cycle in one hour assuming constant irradiation and temperature during simulation for the variable step size algorithm

Figure 16 and 17 show the output power of the solar cell with adaptive algorithm for the second scenario in which the irradiation decreases drastically in the second half of the simulation time.

Figure 18 and 19 show the output power of the solar cell under adaptive algorithm for the third scenario in which the irradiation decrease drastically only for 5 minutes in the whole simulation time.

Table 2 summarizes simulation results by showing the calculated energy efficiency metric introduced in section V.

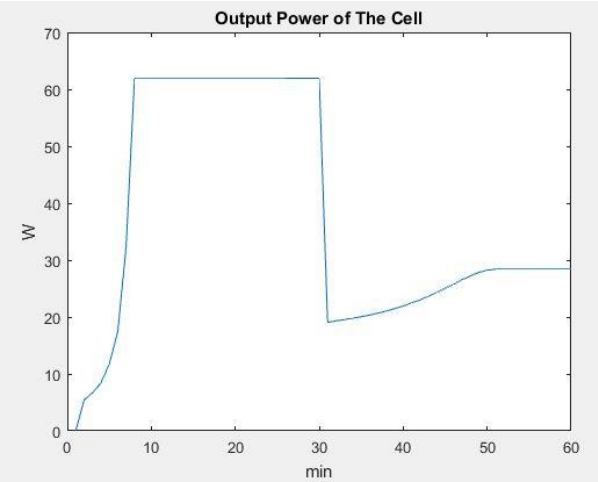

Figure 16: Output power in one hour assuming irradiation cut into half during second half of the simulation for the variable step size algorithm

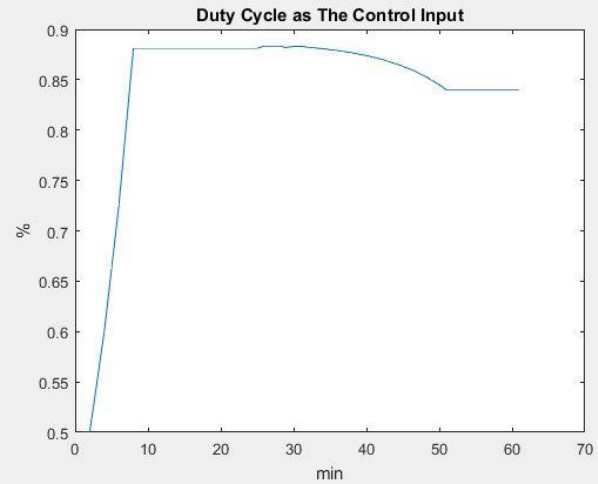

Figure 17: Duty Cycle in one hour assuming constant irradiation and temperature during simulation for the variable step size algorithm

Since this simulation is done for high power generation PV cell, circuit loss is neglected which means P_{circ} in equation 2 is zero. P&O with fixed step size is not efficient for changing environments. Due to fixed step size, oscillation in the maximum power point is inevitable which decreases the overall efficiency. From Table 2 adaptive algorithm reaches 17.75%, 9.19% and 17.24% more efficiency in tracking maximum power point.
In this algorithm there are two factors that increase the average power and therefore efficiency. The first factor is the faster transition. This is due to the capability of the algorithm to revert to big step size for condition change.

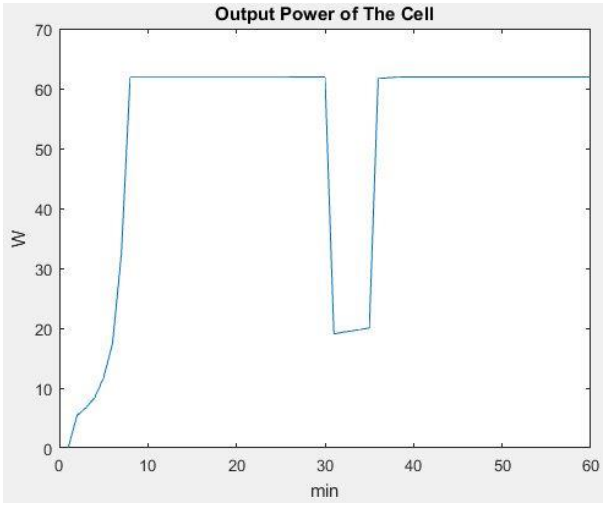

Figure 14.a : Output power in one hour assuming a 5 minute-decrease in the amount of the irradiation during 1 hour of simulation for the variable step size algorithm

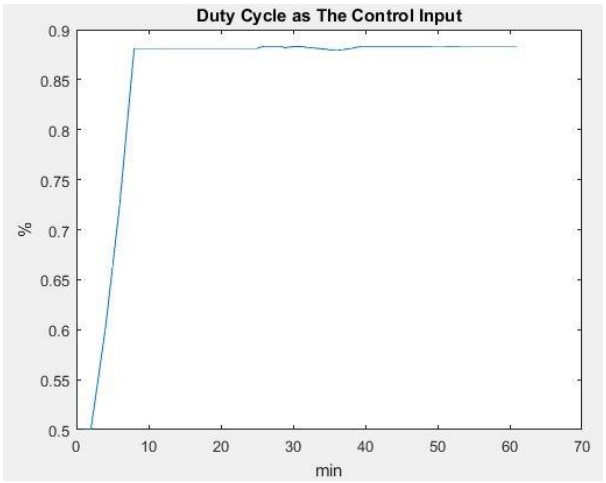

Figure 14.b : Duty Cycle in one hour assuming a 5 minute-decrease in the amount of the irradiation during 1 hour of simulation for the variable step size algorithm

The second factor is small fluctuation when in the maximum power point. In terms of switching activity also adaptive method doesn't show considerable higher switching activity which is desirable in terms of dynamic power dissipation within the control circuit. Bigger step sizes are showing better efficiency in terms of output power. For the applications such as battery charging additional regulator circuitry may be necessary which can make efficiency worse. According to the results adaptive algorithm can be more desired algorithm even though it may need more hardware to be implemented rather than the simple fixed step size algorithm.

Table 2: Energy Efficiency factor for fixed and variable step size algorithm under three different irradiation scenarios.

	Scenario I				Scenario II				Scenario III			
	T_T	Switching Activity	Average Power	Efficiency	T_T	Switching Activity	Average Power	Efficiency	T_T	Switching Activity	Average Power	Efficiency
Fixed Step size, Step=0.025	19	0.8074	44.17	72.67	19	0.7943	28.93	47.59	19	0,8041	41.07	67.57
Fixed Step size, Step=0.05	12	0.8505	38.056	70.24	12	0.8262	27.79	51.28	12	08475	36.36	67.12
Fixed Step size, Step=0.075	9	0.8369	37.56	61.79	9	0.800	27.07	44.53	9	0.8295	34.79	57.24
Fixed Step size, Step=0.1	8	0.8693	32.33	59.67	8	0.8148	23.89	44.09	8	0.8574	31.11	57.42
Variable Step Size	8	0.85	56.01	90.51	8	0.84	37.46	60.47	8	0.85	52.52	84.81

7. CONCLUSION

Power efficiency of the most commercially used algorithms is investigated. The behavior of closed loop fixed and adaptive step size perturb and observe method for solar energy harvesting is simulated using MATLAB. Three different ambient changing condition scenarios are considered. Using the proposed energy efficiency metric adaptive step size algorithm provides higher efficiency of 17.75%, 9.19% and 17.24% more than fixed step size algorithm. In addition adaptive algorithm offers almost zero fluctuation DC output. The only drawback of the adaptive algorithm is more hardware complexity and more cost.

References

[1] Green MA. The path to 25% silicon solar cell efficiency: history of silicon cell evolution. Progress in Photovoltaics: Research and Applications. 2009 May 1;17(3):183-9.

[2] Green MA, Emery K, Hishikawa Y, Warta W, Dunlop ED. Solar cell efficiency tables (Version 45). Progress in photovoltaics: research and applications. 2015 Jan 1;23(1):1-9.

[3] Masoum MA, Dehbonei H, Fuchs EF. Theoretical and experimental analyses of photovoltaic systems with voltage- and current-based maximum power-point tracking. IEEE Transactions on Energy Conversion. 2002 Dec;17(4):514-22.

[4] Salas V, Olias E, Barrado A, Lazaro A. Review of the maximum power point tracking algorithms for stand-alone photovoltaic systems. Solar energy materials and solar cells. 2006 Jul 6;90(11):1555-78.

[5] Houssamo I, Locment F, Sechilariu M. Experimental analysis of impact of MPPT methods on energy efficiency for photovoltaic power systems. International Journal of Electrical Power & Energy Systems. 2013 Mar 31;46:98-107.

[6] Chiang JH, Liu BD, Chen SM, Yang HT. A low supply voltage mixed-signal maximum power point tracking controller for photovoltaic power system. In System-on-Chip Conference (SOCC), 2014 27th IEEE International 2014 Sep 2 (pp. 125-129). IEEE.

[7] Esram T, Chapman PL. Comparison of photovoltaic array maximum power point tracking techniques. IEEE Transactions on energy conversion. 2007 Jun;22(2):439-49

[8] Reisi AR, Moradi MH, Jamasb S. Classification and comparison of maximum power point tracking techniques for photovoltaic system: A review. Renewable and Sustainable Energy Reviews. 2013 Mar 31;19:433-43.

[9] Kamarzaman NA, Tan CW. A comprehensive review of maximum power point tracking algorithms for photovoltaic systems. Renewable and Sustainable Energy Reviews. 2014 Sep 30;37:585-98.

[10] Kivimäki J, Kolesnik S, Sitbon M, Suntio T, Kuperman A. Revisited Perturbation Frequency Design Guideline for Direct Fixed-Step Maximum Power Point Tracking Algorithms. IEEE transactions on industrial electronics. 2017, DOI: 10.1109/TIE.2017.2674589.

[11] Elgendy MA, Zahawi B, Atkinson DJ. Assessment of perturb and observe MPPT algorithm implementation techniques for PV pumping applications. IEEE transactions on sustainable energy. 2012 Jan;3(1):21-33.

[12] Piegari L, Rizzo R. Adaptive perturb and observe algorithm for photovoltaic maximum power point tracking. IET Renewable Power Generation. 2010 Jul 1;4(4):317-28

[13] Aashoor FA, Robinson FV. A variable step size perturb and observe algorithm for photovoltaic

maximum power point tracking. In Universities Power Engineering Conference (UPEC), 2012 47th International 2012 Sep 4 (pp. 1-6). IEEE

[14] Liu F, Duan S, Liu F, Liu B, Kang Y. A variable step size INC MPPT method for PV systems. IEEE Transactions on industrial electronics. 2008 Jul;55(7):2622-8

[15] Ahmed J, Salam Z. An improved perturb and observe (P&O) maximum power point tracking (MPPT) algorithm for higher efficiency. Applied Energy. 2015 Jul 15;150:97-108

[16] Sera D, Teodorescu R, Hantschel J, Knoll M. Optimized maximum power point tracker for fast-changing environmental conditions. IEEE Transactions on Industrial Electronics. 2008 Jul;55(7):2629-37.

[17] Kim H, Kim S, Kwon CK, Min YJ, Kim C, Kim SW. An energy-efficient fast maximum power point tracking circuit in an 800-μW photovoltaic energy harvester. IEEE transactions on power electronics. 2013 Jun;28(6):2927-35

[18] Rahman MW, Bathina C, Karthikeyan V, Prasanth R. Comparative analysis of developed incremental conductance (IC) and perturb & observe (P&O) MPPT algorithm for photovoltaic applications. In Intelligent Systems and Control (ISCO), 2016 10th International Conference on 2016 Jan 7 (pp. 1-6). IEEE

[19] Yu GJ, Jung YS, Choi JY, Kim GS. A novel two-mode MPPT control algorithm based on comparative study of existing algorithms. Solar Energy. 2004 Apr 30;76(4):455-63.

[20] Fermia N, Granozio D, Petrone G, Vitelli M. Predictive & adaptive MPPT perturb and observe method. IEEE Transactions on Aerospace and Electronic Systems. 2007 Jul;43(3).

[21] Petreuş D, Dărăban Ş, Cirstea M, Pătărău T, Etz R. A novel implementation of a maximum power point tracking system with digital control. In Industrial Electronics (ISIE), 2011 IEEE International Symposium on 2011 Jun 27 (pp. 977-982). IEEE.

[22] De Cristofaro M, Femia N, Migliaro M, Petrone G. Minimum computing adaptive MPPT control. InIndustrial Electronics (ISIE), 2014 IEEE 23rd International Symposium on 2014 Jun 1 (pp. 1384-1389). IEEE.

[23] Jiang Y, Qahouq JA, Haskew TA. Adaptive step size with adaptive-perturbation-frequency digital MPPT controller for a single-sensor photovoltaic solar system. IEEE transactions on power Electronics. 2013 Jul;28(7):3195-205.

[24] Ahmad J. A fractional open circuit voltage based maximum power point tracker for photovoltaic arrays. In Software Technology and Engineering (ICSTE), 2010 2nd International Conference on 2010 Oct 3 (Vol. 1, pp. V1-247). IEEE.

[25] Lee JH, Bae H, Cho BH. Advanced incremental conductance MPPT algorithm with a variable step size. In Power Electronics and Motion Control Conference, 2006. EPE-PEMC 2006. 12th International 2006 Aug 30 (pp. 603-607). IEEE.

[26] Alajmi BN, Ahmed KH, Finney SJ, Williams BW. Fuzzy-logic-control approach of a modified hill-climbing method for maximum power point in microgrid standalone photovoltaic system. IEEE Transactions on Power Electronics. 2011 Apr;26(4):1022-30.

[27] Bahgat AB, Helwa NH, Ahmad GE, El Shenawy ET. Maximum power point traking controller for PV systems using neural networks. Renewable Energy. 2005 Jul 31;30(8):1257-68.